Published in final edited form as:
Apoptosis. 2009 October ; 14(10): . doi:10.1007/s10495-009-0393-z.

Partial attenuation of cytotoxicity and apoptosis by SOD1 in ischemic renal epithelial cells

Huan Ling Liang,
Division of Transplant Surgery, Medical College of Wisconsin, Milwaukee, WI 53226, USA, Kidney Disease Center, H4135, Medical College of Wisconsin, 8701 Watertown Plank Road, Milwaukee, WI 53226, USA

Jody Arsenault,
Department of Pharmacology, LSU Health Sciences Center, New Orleans, LA, USA

Jordan Mortensen,
Division of Transplant Surgery, Medical College of Wisconsin, Milwaukee, WI 53226, USA, Kidney Disease Center, H4135, Medical College of Wisconsin, 8701 Watertown Plank Road, Milwaukee, WI 53226, USA

Frank Park,
Kidney Disease Center, H4135, Medical College of Wisconsin, 8701 Watertown Plank Road, Milwaukee, WI 53226, USA, Department of Physiology, Medical College of Wisconsin, Milwaukee, WI 53226, USA, Department of Medicine (Division of Nephrology), Medical College of Wisconsin, Milwaukee, WI 53226, USA

Christopher P. Johnson, and
Division of Transplant Surgery, Medical College of Wisconsin, Milwaukee, WI 53226, USA, Kidney Disease Center, H4135, Medical College of Wisconsin, 8701 Watertown Plank Road, Milwaukee, WI 53226, USA, VA Medical Center, Medical College of Wisconsin, Milwaukee, WI 53226, USA

Vani Nilakantan
Division of Transplant Surgery, Medical College of Wisconsin, Milwaukee, WI 53226, USA, Kidney Disease Center, H4135, Medical College of Wisconsin, 8701 Watertown Plank Road, Milwaukee, WI 53226, USA

Vani Nilakantan: vnilakan@mcw.edu

Abstract

Reactive oxygen species (ROS) contribute significantly to apoptosis in renal ischemia-reperfusion (IR) injury, however the exact mechanisms are not well understood. We used novel lentiviral vectors to over-express superoxide dismutase 1 (SOD1) in proximal tubular epithelial (LLC-PK_1) cells and determined effects of SOD1 following ATP depletion-recovery, used as a model to simulate renal IR. SOD1 over-expression partially protected against cytotoxicity ($P < 0.001$) and decreased superoxide ($O_2^{\bullet -}$) in ATP depleted cells. The ATP depletion-mediated increase in nuclear fragmentation, an index of apoptosis and activation of caspase-3 was also partially blocked by SOD1 ($P < 0.05$). However, SOD1 over-expression was insufficient to completely attenuate caspase-3, indicating that ROS other than cytoplasmic $O_2^{\bullet -}$ are involved in ATP depletion mediated injury. To test the contribution of hydrogen peroxide, a subset of enhanced

Correspondence to: Vani Nilakantan, vnilakan@mcw.edu.
Present Address: J. Arsenault Eli Lilly, Indianapolis, IN, USA

green fluorescent protein (EGFP) and SOD1 (serum free and injured) cells were treated with polyethylene glycol-catalase (PEG-catalase). As expected there was 50% reduction in cytotoxicity and caspase-3 in SOD1 cells compared to EGFP cells; catalase treatment decreased both indices by an additional 28% following ATP depletion. To test the role of mitochondrial derived superoxide, we also treated a subset of LLC-PK_1 cells with the mitochondrial antioxidant, Mito-TEMPO. Treatment with MitoTEMPO also decreased ATP depletion induced cytotoxicity in LLC-PK_1 cells in a dose dependant manner. These studies indicate that both SOD1 dependent and independent pathways are integral in protection against ATP depletion-recovery mediated cytotoxicity and apoptosis, however more studies are needed to delineate the signaling mechanisms involved.

Keywords

Apoptosis; ATP depletion; Catalase; Lentiviral; Reactive oxygen species; SOD1

Introduction

Renal ischemia reperfusion (IR) injury, one of the common sources of acute kidney injury induces severe cytotoxicity in the outer medullary proximal tubules [1, 2]. IR-induced cell injury of polarized renal epithelial cells results in many biochemical, physiological, and morphological alterations [3–5], including decrease in ATP, increased calcium, oxidative stress, membrane lipid peroxidation, and alterations in enzyme activities. The extent of the injury to the tubular epithelial cells is dependent on the length and severity of the ischemic period [6]. Oxidative stress and the generation of reactive oxygen species (ROS) play an important role during renal epithelial injury [7–9]. Whether cells die from ROS-induced apoptosis, however, depends on the balance between the generation of oxidant species and the removal of oxidants by the intracellular antioxidant systems. To protect against the potentially damaging effects of ROS, antioxidant enzymes such as SOD, catalase and glutathione peroxidase play key roles.

Cells have therefore elaborated protective mechanisms against potentially damaging molecules such as ROS by synthesizing antioxidant enzymes [10]. Superoxide dismutases (SODs) play a central role in disproportionating $O_2^{\bullet -}$ into oxygen and H_2O_2 which is further detoxified by glutathione peroxidase or catalase [11]. Copper/Zinc SOD (Cu/Zn SOD or SOD1) contains copper and zinc ions and is constitutively present in the cytosol and mitochondrial intermembrane space of eukaryotic cells [12, 13]. SOD2 contains a manganese ion and is located exclusively in the mitochondrial matrix and SOD3 is mainly extracellular. Of the three SODs, SOD1 is the most abundant in the kidney and thus serves as a major antioxidant system. IR results in the impairment of intracellular antioxidant defenses, particularly SOD1 [14] rendering the cell more susceptible to oxidative stress [15]. Previously, studies have shown the protective effect of SOD2 over-expression in various injury models, including cardiac functional recovery in myocardial IR [16], and markedly increasing the resistance to caspase-mediated apoptosis in in vitro models [17, 18]. Deficiency of SOD1 also increases susceptibility to acute renal failure in mice and adenoviral transfer of SOD1 attenuates IR injury in the kidney [19]. However, the use of adenoviral vector mediated gene transfer has limitations since adenoviral vectors are largely episomal following infection and are not suited for stable transfection and long term studies due to loss of the transgene. The current study was designed to assess the role of SOD1 in a simulated IR injury model in vitro using novel lentiviral vector mediated techniques to over-express SOD1. The lentiviral vectors are stably integrated into the host genome, allowing for stable transgene expression in quiescent and dividing cells in vitro. Porcine LLC-PK_1 proximal tubule cells were transduced using an integrating, non-replicating lentiviral vector

system as previously described by our group [20] to over-express human SOD1. Using these genetically modified LLC-PK_1 cells, an ATP depletion-recovery protocol was performed as previously established [21–23] to examine the effects of increased SOD1 expression on cytotoxicity, $O_2^{\bullet -}$ levels, and apoptosis. In addition, we studied the role of mitochondrial $O_2^{\bullet -}$ and other ROS, such as hydrogen peroxide (H_2O_2), in mediating cytotoxicity following ATP depletion-recovery.

Materials and methods

Construction of lentiviral transfer plasmid containing human SOD1 cDNA

The human SOD1 cDNA was generously provided by Dr. Charles Epstein (University of California at San Francisco), and the SOD1 was PCR amplified using the following specific PCR primers purchased from Integrated DNA Technologies (Coralville, IA). The primers were designed to include *Bam*HI (sense primer) and *Eco*RI (antisense primer) recognition sites (bold) to facilitate cloning into the lentiviral vector transfer plasmid as well as a consensus Kozak sequence (underlined) to optimize SOD1 translation. The primer sequences were as follows: (sense) 5′-TC**GGATCC**GCCACCATGGCGACGAAGGCCGTGTGCGTG-3′; (antisense) 5′-ATC**GAATTC**CTGCAGAAGATTACAGTGTTTAA-3′. The SOD1 PCR product was amplified using standard conditions, digested with *Bam*HI/*Eco*RI, and ligated into the purified *Bam*HI/*Eco*RI-digested lentiviral vector transfer plasmid, pHR(+)cEF1α.GFP.R(−).W(+), to replace the GFP cDNA. The pHR(+)cEF1α.GFP.R(−).W(+) is a modified lentiviral transfer plasmid that contains the elongation factor 1α (EF1α) promoter driving the expression of green fluorescent protein (GFP), and also contains other *cis*-acting DNA elements, such as the central polypurine tract sequence (cppt) and woodchuck post-regulatory element (WPRE) to maximize transduction efficiency [24–26] and transcript stability [27]. The final construct with the SOD1 cDNA was denoted as pHR(+)cEF1αSOD1.R(−).W(+), and the orientation of the insert was determined by restriction enzyme analysis.

Packaging and envelope pseudotype plasmids

pCMVΔR8.74 is the packaging plasmid that provides the expression of the *gag-pol*, *tat* and *rev* genes, and the viral accessory genes have been deleted or attenuated as previously described by Dull et al. [28]. pMD.G is the envelope plasmid and encodes the vesicular stomatitis virus G protein as previously described [29].

Lentiviral vector production

Modified lentiviral vectors were produced by transient plasmid transfection of 293 T cells using a method previously described [20, 30–32]. The modified lentiviral vectors were produced using the following amounts of plasmid DNA: 10 μg transfer plasmid, 6.5 μg packaging plasmid, and 3.5 μg envelope plasmid. Conditioned media was collected at 48 h following plasmid transfection, filtered and frozen at −80ºC. Single channel FACS analysis (Becton Dickinson, Franklin Lakes, NJ) was performed on EGFP-expressing lentiviral vectors and analyzed with the CellQuest program (Version 3.1f; Becton Dickinson) to determine lentiviral vector titer.

Cell culture and vector transduction

LLC-PK_1 (a porcine proximal tubular epithelial cell line) was obtained from the American Type Culture Collection (Rockville, MD) and grown using α-MEM supplemented with glutamine, 10% fetal bovine serum (Invitrogen, Carlsbad, CA). The cells were serially transduced with VSV-G pseudotyped lentiviral vectors expressing either EGFP or SOD1 at

an MOI ~ 40 in the presence of polybrene (8 μg/ml) on a daily basis, and the cells were expanded. The transduction efficiency by the lentiviral vectors was determined using FACS analysis using the LLC-EGFP cells. LLC-EGFP and LLC-SOD1 cells were used to assess the mRNA, protein and functional enzyme activity of the SOD1 by real-time PCR, Western blots and SOD1 enzyme assay respectively.

Real-time quantitative PCR

Total RNA was isolated from transduced GFP and SOD1 cells by RNAeasy Kits (Qiagen Inc., Valencia, CA) according to the manufacturer's instructions. Two micrograms total RNA was treated with DNase I, cDNA was then synthesized using random hexamer primers and SuperScript™ III RNase H-Reverse Transcriptase (Invitrogen) according to the manufacturer's instructions. Real-time quantitative PCRs (RTqPCR) were carried out in Stratagene Mx™ QPCR system (Stratagene, Cedar Creek, TX) using SYBR Green qPCR SuperMix (Invitrogen). The primer sequences are SOD1 Forward: 5′GGAGAGCATTC CATCATTGG 3′; SOD1 Reverse: 5′CAATCACACCAC AAGCCAAG 3′. The PCR conditions were as follows: 95ºC for 30 s, 60ºC for 60 s, 72ºC for 30 s for 40 cycles. GADPH mRNA served as the internal control and the $\Delta\Delta C_T$ method [33] was used for calculating the relative amount of transcripts.

Western blot

Cell pellets from LLC-EGFP and LLC-SOD1 cells were lysed in RIPA lysis buffer with the addition of protease inhibitors. Protein concentration in cell lysates was measured using a protein assay kit from Bio-Rad (Hercules, CA). Twenty five micrograms of protein was run on 12% SDS/PAGE gel and transferred to nitrocellulose membrane. After blocking for 1 h at room temperature, the blots were incubated with one of the following primary antibodies: rabbit anti-cleaved caspase-3 Asp175 at 1:500 (Cell Signaling Technology, Inc. Danvers, MA); mouse anti-GADPH 1:2000 (Chemicon, Temecula, CA); sheep anti-human SOD1 1:1,000 (Calbiochem, San Diego, CA) overnight at 4ºC. After washing, the membranes were probed with secondary goat–anti-rabbit, goat–anti-sheep, or goat–anti-mouse IgG conjugated to horseradish peroxidase (HRP) (Bio-Rad) at 1:10,000 for 1 h at RT. The blots were visualized with ECL-Plus.

SOD activity assay

The activity of SOD from lentiviral vector-transduced LLC-PK_1 cells (LLC-EGFP and LLC-SOD1) was measured using a commercially available SOD assay kit (Cayman Chemical, Ann Arbor, MI). This kit utilizes a tetrazolium salt for detection of $O_2^{\bullet -}$ radicals generated by xanthine oxidase and hypoxanthine. Briefly, the cell pellets (LLC-EGFP and LLC-SOD1) were resuspended in cold 20 mM HEPES buffer (pH 7.2, containing 1 mM EGTA, 210 mM mannitol, and 70 mM sucrose), sonicated for 20 s on ice and then centrifuged at 1,500*g* for 5 min at 4ºC. The absorbance was read at 450 nm according to manufacturer's instructions. The final presentation of SOD activity was unit per microliter per microgram of protein.

ATP depletion-recovery experiments in LLC-EGFP and LLC-SOD1 cells

Both LLC-EGFP and LLC-SOD1 cells were grown in α-MEM containing 10% FBS, 100 U/ml penicillin, 100 μg/ml streptomycin, and 290 μg/ml L-glutamine at 37ºC in a 5% CO_2/95% air humidified incubator. Cells were grown to confluence in six-well plates before initiation of the injury (ATP depletion) and recovery protocols as previously described [20, 22, 23]. On the day of the experiment, cells were rinsed with 37ºC DPBS and incubated in pre-warmed serum free α-MEM 30 min prior to ATP depletion. To achieve ATP depletion, cells were incubated in pre-warmed substrate-free α-MEM with the addition of 0.1 μM

antimycin A. To maintain osmolarity, 5.5 mM of the non-metabolizable form of glucose, L-glucose, was added. Following 2 or 4 h of ATP depletion, the cells were recovered in serum-free α-MEM for 2 h (IM, 2–2 or 4–2 h). At the end of the experiment, media was collected for LDH and cells harvested for protein assay, caspase-3 activity and Western blots. Control cells (SF) were grown in parallel and underwent equivalent washes and incubated in serum-free α-MEM throughout the experiment.

Catalase treatment

Catalase-polyethylene glycol (PEG-Cat, Sigma, St. Louis, MO) at concentrations of 50, 100, 200 and 400 U were initially tested on wild-type LLC-PK_1 cells to determine the effective dose following ATP depletion-recovery. Since PEG-Cat was most effective at 200 U, subsequent experiments were performed using this dose (200 U). A subset of EGFP and SOD1 cells (serum free and IM) were treated with 200 U of PEG-Cat at the beginning of the ATP depletion phase (4 h) and replenished during the recovery phase (2 h) (LLC-Cat). At the end of the experiment, both culture media and cells were harvested for LDH, caspase-3 activity.

MitoTEMPO treatment

MitoTEMPO was purchased from Axxora (San Diego, CA). A subset of wild type LLC-PK_1 cells was treated with mitochondria targeted antioxidant, MitoT EMPO at doses ranging from 1 to 1,000 nM. Cells were then subject to ATP depletion for 4 h followed by recovery in serum free media for 2 h (IM, 4–2 h). At the end of the experiment, culture media was collected for the LDH and caspase-3 activity assay.

Western blot for catalase and SOD2—Approximately 50 μg protein of protein lysate from LLC-EGFP or LLC-SOD1 cells was electrophoresed on either 12% (for SOD2) or 10% (for catalase) SDS–PAGE gels and transferred to PVDF membranes. After blocking for 1 h, the membranes were incubated with either anti-catalase (Santa Cruz Biotechnology, Santa Crux, CA, 1:1,000) or anti SOD2 (Upstate Biotechnology, Lake Placid, NY, 1:1000) overnight at 4ºC. After primary antibody incubations, membranes were washed and incubated with secondary antibodies conjugated to HRP (Bio-Rad, Hercules, CA, 1:10,000) for 1 h and visualized using ECL-Plus.

Determination of cytotoxicity

Cytotoxicity in serum free control (SF) and ATP depleted (IM) lentiviral vector-transduced LLC-PK_1 cells (LLC-EGFP and LLC-SOD1, LLC-Cat) and MitoTEMPO treated cells was measured by the release of lactate dehydrogenase (LDH) into the media using a commercially available kit (Diagnostic Chemicals, Oxford, CT) within 24 h of harvest. This kit is based on the conversion of L-lactate and NAD to pyruvate and NADH by the released LDH. The rate of increase in absorbance of the reaction mixture, from the formation of NADH, at 340 nm is proportional to the LDH activity. The final presentation of LDH was mU per microgram of protein.

Detection of $O_2^{\bullet -}$ levels by DHE staining

Superoxide levels in the lentiviral vector-transduced LLC-PK_1 cells (LLC-EGFP and LLC-SOD1) following either 2–2 or 4–2 h ATP depletion-recovery was determined qualitatively by dihydroethidium (DHE) fluorescence, a specific probe for intracellular $O_2^{\bullet -}$ production. Cells were loaded with 10 μM hydroethidium (HE) 20 min before the end of the experiment. After washing 2 times in PBS, cells were immediately scanned for DHE red fluorescence using an Olympus IX50 inverted microscope (Olympus America, Center Valley, PA) equipped with rhodamine filter settings.

Measurement of $O_2^{\bullet-}$ by HPLC

Intracellular $O_2^{\bullet-}$ was quantitatively measured by high-performance liquid chromatography/fluorescence assay using hydroethidine as previously described [34]. The assay utilizes hydroethidine (HE) as an intracellular probe that reacts with $O_2^{\bullet-}$ to form the reaction product 2-hydroxyethidium (2-OH-E^+). Lentiviral vector-transduced LLC-PK_1 cells (LLC-EGFP and LLC-SOD1) underwent either 2 or 4 h of ATP depletion followed by a 2 h recovery period. Thirty minutes prior to the end of recovery, cells were treated with 10 μM HE. Following the 30-min incubation of HE in the dark, cells were washed one time with cold dPBS, harvested and prepared as followed [34]. One hundred fifty microliters of each sample was injected into the HPLC system (HP 1100, Agilent Technologies, Palo Alto, CA) for HPLC analysis, with fluorescence detection at 510 nm (excitation) and 595 nm (emission). 2-OH-E^+ standard, prepared by reacting HE with Fremy's salts, was generated as previously described [35]. HPLC peak areas were normalized to the protein concentration of cell lysates and reported as nanomole of 2-OH-E^+ per milligram of protein.

H_2O_2 levels

H_2O_2 levels were evaluated in LLC-EGFP and LLC-SOD1 cells with a Amplex® hydrogen peroxide/peroxidase assay kit (Molecular Probes, Eugene, OR) using manufacturer's instructions. In this method, Amplex Red reacts with H_2O_2 in the presence of HRP to produce resorufin, a red fluorescent product. Briefly, samples and standard were incubated with Amplex Red reagent and HRP in the dark for 30 min. The fluorescence was immediately read in fluorescent plate reader with the absorbance set at 571 nm and emission set at 585 nm.

Hoechst 33258 staining

LLC-EGFP and LLC-SOD1 cells were grown on Poly-L-lysine coated glass coverslips. After 4 h of ATP depletion and 2 h of recovery, cells were fixed with pre-chilled phosphate-buffered saline (PBS) containing 4% paraformaldehyde for 30 min at room temperature. Following three washes with PBS, cells were exposed to 1 mg/l fluorescent DNA-binding dye Hoechst 33258 (Sigma, St. Louis, MO) for 15 min at room temperature in the dark. After three washes in PBS, samples were analyzed under a Nikon fluorescent microscope using DAPI filter.

Annexin V flow cytometry

Apoptosis was evaluated in both LLC-EGFP and LLC-SOD1 cells after ATP depletion-recovery by flow cytometry via APC tagged Annexin V staining according to manufacturer's instructions (BD Pharmingen, Franklin Lakes, NJ). APC Annexin V-positive cells were classified as apoptotic. Analyses were performed using FACS Calibur flow cytometer (BD BioSciences, San Jose, CA).

Detection of caspase-3 levels

The levels of caspase-3 activity were measured in protein lysates from serum free (SF) and ATP depleted (IM, 4–2 h) LLC-EGFP, LLC-SOD1 and LLC-Cat and MitoTEMPO treated cells using a commercially available kit (Upstate, Temecula, CA). This kit utilizes the detection of the chromophore *p*-nitroaniline (*p*NA), which is measured spectrophotometrically at 405 nm, after cleavage from labeled substrate *N*-acetyl-Asp–Glu–Val–Asp-*p*NA (DEVD-*p*NA). Released *p*NA was quantified by generating a *p*NA standard curve. Western blot analysis for the activated caspase-3 was performed as another method to determine apoptosis. Thirty micrograms of cellular protein was used and Western Blot performed as described above.

Statistical analysis

Mean values ± SEM are expressed. The significance of differences in mean values was evaluated by one-way ANOVA, followed by a Newman–Keuls multiple comparison test. $P < 0.05$ was considered statistically significant.

Results

Validation of SOD1 expression and activity in genetically modified LLC-PK$_1$ cells using lentiviral vectors

LLC-PK$_1$ cells were serially transduced (MOI ~ 40) with VSV-G pseudotyped lentiviral vectors expressing either EGFP or SOD1 over a 6 days period to ensure that every cell was genetically modified by the lentiviral vector. This genetic modification protocol of the LLC-PK$_1$ cells was recently established in our lab [20]. The LLC-PK$_1$ cells transduced with the EGFP marker were labeled as LLC-EGFP, and the SOD1 expressing cells were labeled LLC-SOD1. FACS analysis was performed on the LLC-EGFP cells demonstrating extremely high transduction (>99%; $n = 6$ experiments) as shown in Fig. 1a. Expression of SOD1 mRNA was increased significantly compared to control LLC-EGFP cells (Fig. 1b, $P < 0.01$ EGFP vs. SOD1), and this increase in SOD1 mRNA corresponded with higher levels of SOD1 immunoreactive protein (Fig. 1c) and functional SOD activity (Fig. 1d, $P < 0.05$ EGFP vs. SOD1). SOD1 over-expression did not affect expression of the mitochondrial $O_2^{\bullet -}$ scavenging protein, SOD2 (Fig. 1e). Catalase protein was very slightly decreased in the SOD1 over-expressing cells compared to the EGFP expressing cells (Fig. 1e).

Determination of cytotoxicity in LLC-EGFP, LLC-SOD1 cells following ATP depletion and recovery

Cytotoxicity was measured by the amount of LDH released from the LLC-SOD1 and LLC-EGFP cells into the media following a 2 h period of ATP depletion with a subsequent 2 h recovery period (2–2 h IM). Following the 2–2 h IM treatment, no significant increase in cytotoxicity ($P > 0.05$) was detected in EGFP or SOD cells compared to serum-free controls (Fig. 2a). Using a more prolonged ATP depletion phase (4–2 h instead of 2–2 h), we found that the levels of LDH was significantly increased ($P < 0.001$ EGFP SF vs. EGFP IM) in LLC-EGFP group (10.17 ± 0.93 mU/mg protein) compared to serum-free controls (3.05 ± 0.49 mU/mg protein). In contrast, Fig. 2b shows that SOD1 over-expression in LLC-PK$_1$ cells resulted in 50% attenuation in LDH release following injury (Fig. 2b, $P < 0.001$ SOD IM vs. EGFP IM). However, the protective effect of SOD1 was only partial, since cytotoxicity in SOD1 IM cells was still significantly higher compared to its serum-free controls (Fig. 2b, P < 0.05 SOD SF vs. SOD IM).

SOD1 over-expression partially decreases $O_2^{\bullet -}$ following ATP depletion-recovery at the early time point of ATP depletion-recovery

Light microscopic images indicated that SOD1 over-expression did not decrease the total number of cells following ATP depletion-recovery compared to LLC-EGFP (Fig. 3, upper panel). Following the 2–2 h ATP depletion-recovery period, qualitative assessment of $O_2^{\bullet -}$ in live LLC-EGFP and LLC-SOD1 cells showed very low levels of $O_2^{\bullet -}$ in both LLC-EGFP and LLC-SOD1 under serum-free conditions by DHE fluorescence imaging (Fig. 3a, lower panel-serum free). $O_2^{\bullet -}$ levels were increased in LLC-EGFP following 2–2 h ATP depletion-recovery (Fig. 3a, lower panel, EGFP-IM), whereas the LLC-SOD1 cells were found to have lower $O_2^{\bullet -}$ levels, although SOD1 over-expression did not completely abolish the presence of $O_2^{\bullet -}$ in the cells (Fig. 3, lower panel, SOD1-IM) as compared to the serum-free control cells.

Intracellular $O_2^{\bullet-}$ level was also measured by HPLC using HE as a probe in both LLC-EGFP and LLC-SOD1 cells after 2–2 and 4–2 h ATP depletion-recovery. SOD1 over-expression partially decreased $O_2^{\bullet-}$ in both serum free (EGFP, 0.02 ± 0.01 nmol/mg protein vs. SOD1, 0.01 ± 0.0001 nmol/mg protein) and injured (EGFP, 0.04 ± 0.005 nmol/mg protein vs. SOD1, 0.03 ± 0.003 nmol/mg protein) groups compared to LLC-EGFP controls (Fig. 3b, $P < 0.05$ EGFP IM vs. EGFP serum free and SOD1 serum free) although not to levels seen in control cells. Following longer durations of ATP depletion-recovery (4–2 h), there was a substantial increase in $O_2^{\bullet-}$ in EGFP cells (EGFP serum free, 0.04 ± 0.008 nmol/mg protein vs. EGFP IM, 0.12 ± 0.003 nmol/mg protein). The ATP depletion mediated increase in $O_2^{\bullet-}$ was specific because addition of a cell permeable SOD mimetic, MnTMPyP completely blocked $O_2^{\bullet-}$ levels (0.032 ± 0.003 nmol/mg protein). Surprisingly, SOD1 over-expression did not attenuate $O_2^{\bullet-}$ at this time point (SOD1 serum free, 0.034 ± 0.01 nmol/mg protein vs. SOD IM, 0.13 ± 0. 01 nmol/mg protein).

Effect of SOD1 over-expression on H_2O_2 levels following ATP depletion-recovery

We next examined whether increase in SOD1 expression resulted in an increase in H_2O_2 by Amplex Red fluorescence. There was a slight increase in H_2O_2 following ATP depletion-recovery in the EGFP cells (Fig. 3c). Interestingly, and contrary to our expectations, in SOD1 cells, H_2O_2 levels were not increased to the same extent as in EGFP cells (Fig. 3c).

SOD1 over-expression partially prevents nuclear fragmentation following ATP depletion-recovery

We used Hoechst nuclear staining to analyze the nuclear morphology in LLC-EGFP and LLC-SOD1 cells following ATP depletion-recovery. Under serum free conditions, both LLC-EGFP and LLC-SOD1 displayed normal nuclear morphology (Fig. 4a). There was increased nuclear condensation and fragmentation of nuclei in EGFP-ATP depleted cells (depicted by yellow arrows in Fig. 4a) compared to the LLC-SOD1 treated under ATP depleted conditions. There was some evidence of nuclear damage in the SOD1-expressing cells (Fig. 4a), but the numbers were vastly lower than the EGFP-expressing cells.

Further, we used Annexin V flow cytometry to determine the effect of SOD1 over-expression on apoptosis following ATP depletion-recovery. As shown in Fig. 4b, there was an increase in Annexin V staining in EGFP cells following 4 h of ATP depletion and 2 h of recovery ($P < 0.01$ serum free vs. IM). This was partially decreased by SOD1 over-expression although the results did not reach a statistical significance (Fig. 4b).

SOD1 over-expression partially decreases activation of caspase-3 following ATP depletion-recovery

To assess the role of SOD1 in regulating the apoptotic signaling pathway, we examined caspase-3, an effector protease in the apoptotic signaling cascade, following 4–2 h ATP depletion-recovery in LLC-EGFP and LLC-SOD1 cells. First, Western blot analysis was used to determine the functional activity of caspase-3 detecting its cleavage products (17- and 20-kDa bands) using a specific antibody. Under serum-free conditions, functional caspase-3 was not detectable by Western blot analysis in both LLC-EGFP and LLC-SOD1 cells (Fig. 5a). However, following ATP depletion-recovery (4–2 h IM) there was a marked increase in activated caspase-3 (17 kDa band) in LLC-EGFP cells (Fig. 5a), whereas activated caspase-3 in LLC-SOD1 cells was barely detectable.

In order to confirm that this protease was activated in our injury model, we performed a caspase-3 activity assay. Following 4–2 h ATP depletion-recovery, there was significantly increased ($P < 0.001$) caspase-3 activity in LLC-EGFP cells compared to serum-free treated cells (Fig. 5b). SOD1 over-expression was able to significantly ($P < 0.05$ EGFP IM vs.

SOD1 IM) attenuate caspase-3 activity by about 50% compared to the LLC-EGFP cells following 4–2 h IM (Fig. 5b), although the caspase-3 activity was still significantly higher ($P < 0.01$, SOD1 IM vs. SOD1 serum free) compared to the LLC-SOD1 serum-free treated cells. The fact that caspase-3 activity was not completely attenuated by SOD1 over-expression although activated caspase-3 protein was non-detectable in SOD1 cells may have to do with the difference in sensitivity of the two techniques.

Effect of SOD1 + catalase on cytotoxicity and caspase-3 activity in ATP depleted LLC-PK$_1$ cells

Because SOD1 over-expression did not completely block caspase-3 activation, we next tested the possibility that ROS other than $O_2^{\bullet -}$, such as H_2O_2, may also be involved in mediating the cytotoxic response and caspase-3 activation following ATP depletion-recovery. In order to do this, we treated a set of wild-type LLC-PK$_1$ cells with varying doses of polyethylene glycol-catalase (PEG-Cat) ranging from 50 to 400 U to determine the effective dose of catalase that could decrease ATP depletion mediated cytotoxicity. The most effective dose was 200 U, and so this was the dose used in all of our subsequent experiments (data not shown). A subset of LLC-EGFP and LLC-SOD1 cells (serum free and IM) were treated with 200 U of PEG-Cat (designated as LLC-Cat) at the beginning of the ATP depletion phase (4 h) and replenished during the recovery phase (2 h). The addition of catalase to LLC-EGFP cells (Cat IM) also reduced cytotoxicity compared to ATP depleted cells (EGFP IM; Fig. 6a, $P < 0.001$ Cat IM vs. EGFP IM). When catalase was added to the LLC-SOD1 cells (SOD1 + Cat) LDH levels were lower than SOD1 alone (SOD1 IM) although it was not statistically significant as analyzed by the Newman–Keuls multiple comparison test (Fig. 6a).

Caspase-3 activity in EGFP, SOD1, catalase and SOD1 + catalase cells (serum free and IM) showed trends similar to the observed cytotoxicity following ATP depletion-recovery (Fig. 6b). The addition of catalase (Cat IM) to LLC-EGFP cells had a more pronounced attenuation of caspase-3 activity following ATP depletion-recovery (Fig. 6b, $P < 0.01$ Cat IM vs. EGFP IM). The addition of catalase to SOD1 cells (SOD + Cat) had a tendency to decrease caspase-3 activity further although it did not reach statistical significance (Fig. 6b).

To further test whether mitochondrially derived reactive oxygen is critical to tubular cytotoxicity in ischemia, we treated a subset of wild type LLC-PK$_1$ cells (serum free and injured) with varying doses (1–1,000 nM) of a mitochondria-targeted antioxidant, MitoTEMPO. MitoTEMPO was effective in reducing ATP depletion-induced cytotoxicity in a dose dependant manner (Fig. 7a). Further, MitoTEMPO was also able to attenuate caspase-3 activation following ATP depletion-recovery (Fig. 7b). These results indicated that both cytosolic and mitochondrial sources of $O_2^{\bullet -}$ are critical to injury following ATP depletion-recovery in renal epithelial cells.

Discussion

The present study documents the effects of SOD1 over-expression in an in vitro model of ATP depletion injury using novel lentiviral vector techniques to modify SOD1. To our knowledge, this is the first report using lentiviral vector mediated over-expression of SOD1 in renal epithelial cells to examine the effects of ATP depletion-recovery. The main findings of this study were the following: (1) SOD1 over-expression partially prevented cytotoxicity in LLC-PK$_1$ cells following ATP depletion-recovery; (2) there was decreased nuclear fragmentation in SOD1 cells compared to EGFP cells following ATP depletion-recovery; (3) SOD1 over-expression partially attenuated caspase-3 activation; (4) the addition of catalase attenuated cytotoxicity and caspase-3 further, although catalase did not have significant synergistic protective effects with SOD1 and (5) the mitochondrially targeted

antioxidant, MitoTEMPO was also effective in reducing cytotoxicity and caspase-3 activation in ATP depleted renal epithelial cells.

We achieved greater than 99% transduction efficiency by using the VSV-G pseudotyped replication-defective lentiviral vectors thus demonstrating this extremely efficient method of transducing LLC-PK_1 cells. Further, we have shown an increase in SOD1 mRNA and protein using the lentiviral mediated transduction technique. There was also a corresponding increase in SOD1 activity in SOD1 over-expressing cells compared to EGFP although the levels were not as high as shown by the Western blot. This discrepancy in the protein versus activity levels could possibly be due to some posttranslational modification of the SOD1 protein in the transduced cells. Lentiviral vector are distinctly advantageous over other vectors currently in use, e.g., adenoviral vectors. Unlike adenoviral vectors which remain largely episomal, lentiviral vectors are integrated into the host genome. This ability allows for long term, stable transgene expression by lentiviral transduction compared to other viral vectors where there is a rapid loss of transgene expression. To our knowledge, this is the first report demonstrating the use of lentiviral vector mediated over-expression of SOD1 in LLC-PK_1 cells.

Cytotoxicity evoked by the massive formation of radicals, $NO^{\bullet}$ or $O_2^{\bullet-}$, can be ascribed to apoptosis or necrosis, two defined features of the cell death program [36]. Necrosis is regarded as accidental cell death [37] with characteristic signs of cell swelling, membrane rupture, randomly digested DNA and cell dissolution [38]. On the other hand, apoptosis is a regulated process with cells shrinking, chromatin condensation and DNA fragmentation. Whether cells undergo apoptosis or necrosis is dependant on ATP content [39–41].

Our finding in the current study that 2–2 h ATP depletion-recovery did not increase cytotoxicity significantly over serum free controls is in agreement with previously published reports from our laboratory [22, 23]. Following longer duration of (4 h) of ATP depletion in vitro however, there was an increase in cytotoxicity that was partially attenuated by SOD1. SOD1 is the major $O_2^{\bullet-}$-disproportionating enzyme in the proximal tubular cells and thus it is likely that it contributes partially to the cellular protective effects following ATP depletion-recovery. However, SOD1 was not able to decrease LDH levels down to levels observed in serum free controls indicating that other radicals and mitochondrial sources of $O_2^{\bullet-}$ are also involved in injury. In this regard, it has been previously shown that over-expression of the mitochondrial SOD2 (Mn SOD) prevents cell death [42] and protects against IR injury in heart, liver or brain tissues [16, 43–45]. The second caveat with this model of injury is that it does not truly represent in vivo ischemia-reperfusion (IR) injury. It is important to note that other investigators have successfully used hypoxia-reoxygenation of proximal tubular cells as a surrogate model of IR [46, 47]. Future studies in our laboratory will also examine the role of SOD1 over-expression in a model of hypoxia-reoxygenation injury.

We also measured $O_2^{\bullet-}$ levels by DHE fluorescence to determine whether SOD1 over-expression was sufficient to decrease ATP depletion-mediated increases in $O_2^{\bullet-}$. Although SOD1 over-expression decreased $O_2^{\bullet-}$ following earlier time points of injury, the $O_2^{\bullet-}$ levels in injured LLC-SOD1 cells were higher than the serum free controls. Following 4–2 h ATP depletion-recovery, SOD1 over-expression did not impact $O_2^{\bullet-}$ levels. This result was not surprising to us because it is possible that at the longer time point of injury, $O_2^{\bullet-}$ is increased to a maximal level, which SOD1 is unable to scavenge. Additionally it may be due to the likely activation of inner mitochondrial sources of $O_2^{\bullet-}$ in our model of injury against which SOD1 is ineffective.

It has also been previously shown that ATP depletion increases potassium influx due to increase in activity of mitochondrial potassium ATP sensitive channels resulting in increased ROS in mitochondrial matrix and release of H_2O_2 in the cytoplasm [48]. Further, antimycin A increases superoxide both in the matrix and extra mitochondrial space which can be trapped by mitochondrial scavengers and SOD1. Because the substrate deprivation is only for a short period of time (4 h), there are residual substrates available for mitochondria to use and programmed cell death can occur as energy dependant process. Alternatively, cells could die from energy independent mechanisms such as necrosis. Thus, the above processes (ATP depletion and antimycin A) both would release ROS ($O_2^{\bullet -}$and H_2O_2) into the cellular cytoplasm where they can be scavenged by SOD1 and catalase.

Initiation of the death program is achieved by a wide variety of stimuli, with the identification of gene products that positively or negatively modulate the progression of the cell suicide pathway [49]. Both the intrinsic (mitochondrial) and extrinsic (receptor) mediated pathways of apoptosis lead to caspase activation. In its active form, caspase-3, the effector protease of apoptosis plays a role in the proteolytic cleavage of proteins, such as the cleavage of nuclear DNA repair enzyme poly (ADP-ribose) polymerase and inhibitor of caspase-activated DNase [50]. There is increasing evidence indicating that ROS and reactive nitrogen species (RNS) contribute to mitochondrial dysfunction and signal the activation of caspase-3 and initiation of cell death [51, 52]. Our results demonstrated that active caspase-3 expression was increased more in LLC-EGFP than LLC-SOD1 cells in response to ATP depletion injury, suggesting that over-expression of SOD1 partially reduces the severity of caspase-3 activation. However, SOD1 over-expression did not completely block caspase-activation following ATP depletion-recovery. Since SOD1 is most effective in scavenging of cytosolic $O_2^{\bullet -}$ it is likely that other ROS such as H_2O_2 and mitochondrial $O_2^{\bullet -}$ also plays a significant role in caspase-3 activation in our model of injury. To partly address this issue, we treated wild type LLC-PK_1 cells with a mitochondrial antioxidant, MitoTEMPO. These results indicated that low doses of MitoTEMPO were indeed effective in reducing ATP depletion mediated cytotoxicity and apoptosis. At the highest dose, however MitoTEMPO was ineffective against ATP depletion induced cytotoxicity. It is possible that at higher doses, MitoTEMPO exhibits non-specific effects. Further, this finding was consistent with previously published studies that other mitochondrially targeted antioxidants such as MitoQ can result in increased H_2O_2 production at higher doses[53]. In this regard, it is possible that in addition to $O_2^{\bullet -}$, other free radicals such as H_2O_2 also play an important in ATP depletion induced cytotoxicity. Recent studies have suggested that hydroperoxide produced by SOD1 in mitochondrial intermembrane space controls cytochrome *c* catalyzed peroxidation [54], leading to the production of H_2O_2. In fact, neonatal mice over-expressing SOD1 have more hydroperoxide accumulation following ischemia compared to wild type mice [55] and menadione treatment increases DCF fluorescence (an indicator of hydroperoxide) and cell death in SOD1 transgenic neurons compared to wild type neurons [56]. Appropriate concentration of catalase has been shown to be protective in menadione toxicity [57] and VUB induced apoptosis in normal human keratinocytes [58]. Concurrent with these reports, in our study, addition of PEG-catalase to ATP depleted LLC-EFP cells significantly decreased cytotoxicity and caspase-3 activation. When catalase was added to the ATP depleted LLC-SOD1 cells, there was a trend for lower cytotoxicity and apoptosis in SOD1 + catalase cells, although this was not statistically significant. In our protocol, we added PEG-catalase at the beginning of the ATP depletion phase and replenished it during the recovery phase. Thus, it is likely that we may have encountered some loss of catalase during the experiment. So, to elucidate the synergistic protective effects of catalase and SOD1 ATP depletion-recovery, in future studies, it may be necessary to co-transduce SOD1 and catalase together by lentiviral vector mediated techniques to continuously increase the activity of catalase in proximal tubular epithelial cells.

In conclusion, these studies show for the first time that lentiviral vector mediated SOD1 over-expression is able to partially attenuate ATP depletion mediated cytotoxicity and caspase-3 activation in proximal tubular epithelial cells. However, it is likely that multiple signaling molecules such as H_2O_2 are also involved in ATP depletion mediated injury. Future studies will thus utilize genetic techniques to manipulate SOD1 vs. SOD2 and catalase (over-expression and silencing) in vitro to dissect the apoptotic signaling pathways involved.

Acknowledgments

We greatly appreciate the gift of human SOD1 cDNA from Dr. Charles Epstein (University of California, San Francisco). We are also grateful to Dr. Balaraman Kalyanaraman, Jacek Zielonka and the Free Radical Research Center at the Medical College of Wisconsin for help with measurement of 2-OH-E^+. This work was supported in part by a pilot and feasibility project in an NIH P50 (1DK-079306-01), an American Heart Association-Scientist Development Grant (0930326G) and departmental funds to V. Nilakantan.

Abbreviations

EGFP	Enhanced green fluorescent protein
IM	Injury media
IR	Ischemia-reperfusion
LDH	Lactate dehydrogenase
PBS	Phosphate-buffered saline
ROS	Reactive oxygen species
SOD	Superoxide dismutase

References

1. Bonventre JV. Mechanisms of ischemic acute renal failure. Kidney Int. 1993; 43:1160–1178. [PubMed: 8510397]
2. Sutton TA, Molitoris BA. Mechanisms of cellular injury in ischemic acute renal failure. Semin Nephrol. 1998; 18:490–497. [PubMed: 9754601]
3. Venkatachalam MA, Jones DB, Rennke HG, Sandstrom D, Patel Y. Mechanism of proximal tubule brush border loss and regeneration following mild renal ischemia. Lab Invest. 1981; 45:355–365. [PubMed: 7300248]
4. Molitoris BA. Ischemia-induced loss of epithelial polarity: potential role of the actin cytoskeleton. Am J Physiol. 1991; 260:F769–F778. [PubMed: 2058700]
5. Kellerman PS, Bogusky RT. Microfilament disruption occurs very early in ischemic proximal tubule cell injury. Kidney Int. 1992; 42:896–902. [PubMed: 1453583]
6. Kellerman PS, Clark RA, Hoilien CA, Linas SL, Molitoris BA. Role of microfilaments in maintenance of proximal tubule structural and functional integrity. Am J Physiol. 1990; 259:F279–F285. [PubMed: 2386206]
7. Weight SC, Bell PR, Nicholson ML. Renal ischaemia—reperfusion injury. Br J Surg. 1996; 83:162–170. [PubMed: 8689154]
8. Nath KA, Norby SM. Reactive oxygen species and acute renal failure. Am J Med. 2000; 109:665–678. [PubMed: 11099687]
9. Lameire N, Vanholder R. Pathophysiologic features and prevention of human and experimental acute tubular necrosis. J Am Soc Nephrol. 2001; 12(Suppl 17):S20–S32. [PubMed: 11251028]
10. Sies H. Strategies of antioxidant defense. Eur J Biochem. 1993; 215:213–219. [PubMed: 7688300]
11. Fridovich I. Superoxide radical and superoxide dismutases. Annu Rev Biochem. 1995; 64:97–112. [PubMed: 7574505]

12. Okado-Matsumoto A, Fridovich I. Subcellular distribution of superoxide dismutases (SOD) in rat liver: Cu, Zn-SOD in mitochondria. J Biol Chem. 2001; 276:38388–38393. [PubMed: 11507097]
13. Sturtz LA, Diekert K, Jensen LT, Lill R, Culotta VC. A fraction of yeast Cu, Zn-superoxide dismutase and its metallochaperone, CCS, localize to the intermembrane space of mitochondria. A physiological role for SOD1 in guarding against mitochondrial oxidative damage. J Biol Chem. 2001; 276:38084–38089. [PubMed: 11500508]
14. Davies SJ, Reichardt-Pascal SY, Vaughan D, Russell GI. Differential effect of ischaemia-reperfusion injury on anti-oxidant enzyme activity in the rat kidney. Exp Nephrol. 1995; 3:348–354. [PubMed: 8528679]
15. Jassem W, Fuggle SV, Rela M, Koo DD, Heaton ND. The role of mitochondria in ischemia/reperfusion injury. Transplantation. 2002; 73:493–499. [PubMed: 11889418]
16. Chen Z, Siu B, Ho YS, et al. Overexpression of MnSOD protects against myocardial ischemia/reperfusion injury in transgenic mice. J Mol Cell Cardiol. 1998; 30:2281–2289. [PubMed: 9925365]
17. Cruthirds DL, Saba H, MacMillan-Crow LA. Overex-pression of manganese superoxide dismutase protects against ATP depletion-mediated cell death of proximal tubule cells. Arch Biochem Biophys. 2005; 437:96–105. [PubMed: 15820221]
18. Xiang N, Zhao R, Zhong W. Sodium selenite induces apoptosis by generation of superoxide via the mitochondrial-dependent pathway in human prostate cancer cells. Cancer Che-mother Pharmacol. 2009; 63:351–362.
19. Yin M, Wheeler MD, Connor HD, et al. Cu/Zn-superoxide dismutase gene attenuates ischemia-reperfusion injury in the rat kidney. J Am Soc Nephrol. 2001; 12:2691–2700. [PubMed: 11729238]
20. Nilakantan V, Maenpaa C, Jia G, Roman RJ, Park F. 20-HETE-mediated cytotoxicity and apoptosis in ischemic kidney epithelial cells. Am J Physiol Renal Physiol. 2008; 294:F562–F570. [PubMed: 18171997]
21. Van Why SK, Mann AS, Ardito T, et al. Hsp27 associates with actin and limits injury in energy depleted renal epithelia. J Am Soc Nephrol. 2003; 14:98–106. [PubMed: 12506142]
22. Nilakantan V, Liang H, Maenpaa CJ, Johnson CP. Differential patterns of peroxynitrite mediated apoptosis in proximal tubular epithelial cells following ATP depletion recovery. Apoptosis. 2008; 13:621–633. [PubMed: 18357533]
23. Maenpaa CJ, Shames BD, Van Why SK, Johnson CP, Nilakantan V. Oxidant-mediated apoptosis in proximal tubular epithelial cells following ATP depletion and recovery. Free Radic Biol Med. 2008; 44:518–526. [PubMed: 17997382]
24. Follenzi A, Ailles LE, Bakovic S, Geuna M, Naldini L. Gene transfer by lentiviral vectors is limited by nuclear translocation and rescued by HIV-1 pol sequences. Nat Genet. 2000; 25:217–222. [PubMed: 10835641]
25. Park F, Kay MA. Modified HIV-1 based lentiviral vectors have an effect on viral transduction efficiency and gene expression in vitro and in vivo. Mol Ther. 2001; 4:164–173. [PubMed: 11545606]
26. Zennou V, Petit C, Guetard D, et al. HIV-1 genome nuclear import is mediated by a central DNA flap. Cell. 2000; 101:173–185. [PubMed: 10786833]
27. Zufferey R, Donello JE, Trono D, Hope TJ. Woodchuck hepatitis virus posttranscriptional regulatory element enhances expression of transgenes delivered by retroviral vectors. J Virol. 1999; 73:2886–2892. [PubMed: 10074136]
28. Dull T, Zufferey R, Kelly M, et al. A third-generation lentivirus vector with a conditional packaging system. J Virol. 1998; 72:8463–8471. [PubMed: 9765382]
29. Naldini L, Blomer U, Gallay P, et al. In vivo gene delivery and stable transduction of nondividing cells by a lentiviral vector. Science. 1996; 272:263–267. [PubMed: 8602510]
30. Oh T, Bajwa A, Jia G, Park F. Lentiviral vector design using alternative RNA export elements. Retrovirology. 2007; 4:38. [PubMed: 17550606]
31. Park F, Ohashi K, Kay MA. The effect of age on hepatic gene transfer with self-inactivating lentiviral vectors in vivo. Mol Ther. 2003; 8:314–323. [PubMed: 12907154]

32. Park F, Ohashi K, Chiu W, Naldini L, Kay MA. Efficient lentiviral transduction of liver requires cell cycling in vivo. Nat Genet. 2000; 24:49–52. [PubMed: 10615126]
33. Livak KJ, Schmittgen TD. Analysis of relative gene expression data using real-time quantitative PCR and the 2(-delta delta C(T)) method. Methods. 2001; 25:402–408. [PubMed: 11846609]
34. Zielonka J, Vasquez-Vivar J, Kalyanaraman B. Detection of 2-hydroxyethidium in cellular systems: a unique marker product of superoxide and hydroethidine. Nat Protoc. 2008; 3:8–21. [PubMed: 18193017]
35. Zielonka J, Vasquez-Vivar J, Kalyanaraman B. The confounding effects of light, sonication, and Mn(III)TBAP on quantitation of superoxide using hydroethidine. Free Radic Biol Med. 2006; 41:1050–1057. [PubMed: 16962930]
36. MacMicking J, Xie QW, Nathan C. Nitric oxide and macrophage function. Annu Rev Immunol. 1997; 15:323–350. [PubMed: 9143691]
37. Walker NI, Harmon BV, Gobe GC, Kerr JF. Patterns of cell death. Methods Achiev Exp Pathol. 1988; 13:18–54. [PubMed: 3045494]
38. Wyllie AH, Kerr JF, Currie AR. Cell death: the significance of apoptosis. Int Rev Cytol. 1980; 68:251–306. [PubMed: 7014501]
39. Hiura TS, Li N, Kaplan R, et al. The role of a mitochondrial pathway in the induction of apoptosis by chemicals extracted from diesel exhaust particles. J Immunol. 2000; 165:2703–2711. [PubMed: 10946301]
40. Comelli M, Di Pancrazio F, Mavelli I. Apoptosis is induced by decline of mitochondrial ATP synthesis in erythroleukemia cells. Free Radic Biol Med. 2003; 34:1190–1199. [PubMed: 12706499]
41. Atlante A, Giannattasio S, Bobba A, et al. An increase in the ATP levels occurs in cerebellar granule cells en route to apoptosis in which ATP derives from both oxidative phosphorylation and anaerobic glycolysis. Biochim Biophys Acta. 2005; 1708:50–62. [PubMed: 15949983]
42. Zhong W, Yan T, Webber MM, Oberley TD. Alteration of cellular phenotype and responses to oxidative stress by manganese superoxide dismutase and a superoxide dismutase mimic in RWPE-2 human prostate adenocarcinoma cells. Antioxid Redox Signal. 2004; 6:513–522. [PubMed: 15130278]
43. Keller JN, Kindy MS, Holtsberg FW, et al. Mitochondrial manganese superoxide dismutase prevents neural apoptosis and reduces ischemic brain injury: suppression of peroxynitrite production, lipid peroxidation, and mitochondrial dysfunction. J Neurosci. 1998; 18:687–697. [PubMed: 9425011]
44. Zhou W, Zhang Y, Hosch MS, et al. Subcellular site of superoxide dismutase expression differentially controls AP-1 activity and injury in mouse liver following ischemia/reperfusion. Hepatology. 2001; 33:902–914. [PubMed: 11283855]
45. Mattson MP, Goodman Y, Luo H, Fu W, Furukawa K. Activation of NF-kappaB protects hippocampal neurons against oxidative stress-induced apoptosis: evidence for induction of manganese superoxide dismutase and suppression of peroxynitrite production and protein tyrosine nitration. J Neurosci Res. 1997; 49:681–697. [PubMed: 9335256]
46. Iwata M, Myerson D, Torok-Storb B, Zager RA. An evaluation of renal tubular DNA laddering in response to oxygen deprivation and oxidant injury. J Am Soc Nephrol. 1994; 5:1307–1313. [PubMed: 7893995]
47. Zager RA, Iwata M, Burkhart KM, Schimpf BA. Post-ischemic acute renal failure protects proximal tubules from O2 deprivation injury, possibly by inducing uremia. Kidney Int. 1994; 45:1760–1768. [PubMed: 7933824]
48. Doughan AK, Harrison DG, Dikalov SI. Molecular mechanisms of angiotensin II-mediated mitochondrial dysfunction: linking mitochondrial oxidative damage and vascular endothelial dysfunction. Circ Res. 2008; 102:488–496. [PubMed: 18096818]
49. Schwartzman RA, Cidlowski JA. Apoptosis: the biochemistry and molecular biology of programmed cell death. Endocr Rev. 1993; 14:133–151. [PubMed: 8325248]
50. Matsuu M, Shichijo K, Okaichi K, et al. The protective effect of fermented milk kefir on radiation-induced apoptosis in colonic crypt cells of rats. J Radiat Res (Tokyo). 2003; 44:111–115. [PubMed: 13678339]

51. Metodiewa D, Koska C. Reactive oxygen species and reactive nitrogen species: relevance to cyto(neuro)toxic events and neurologic disorders. An overview. Neurotox Res. 2000; 1:197–233. [PubMed: 12835102]

52. Kitazawa M, Wagner JR, Kirby ML, Anantharam V, Kanthasamy AG. Oxidative stress and mitochondrial-mediated apoptosis in dopaminergic cells exposed to methylcyclopentadienyl manganese tricarbonyl. J Pharmacol Exp Ther. 2002; 302:26–35. [PubMed: 12065696]

53. Doughan AK, Dikalov SI. Mitochondrial redox cycling of mitoquinone leads to superoxide production and cellular apoptosis. Antioxid Redox Signal. 2007; 9:1825–1836. [PubMed: 17854275]

54. Goldsteins G, Keksa-Goldsteine V, Ahtoniemi T, et al. Deleterious role of superoxide dismutase in the mitochondrial intermembrane space. J Biol Chem. 2008; 283:8446–8452. [PubMed: 18171673]

55. Fullerton HJ, Ditelberg JS, Chen SF, et al. Copper/zinc superoxide dismutase transgenic brain accumulates hydrogen peroxide after perinatal hypoxia ischemia. Ann Neurol. 1998; 44:357–364. [PubMed: 9749602]

56. Ying W, Anderson CM, Chen Y, et al. Differing effects of copper, zinc superoxide dismutase overexpression on neurotoxicity elicited by nitric oxide, reactive oxygen species, and excitotoxins. J Cereb Blood Flow Metab. 2000; 20:359–368. [PubMed: 10698074]

57. Sun JS, Tsuang YH, Huang WC, et al. Menadione-induced cytotoxicity to rat osteoblasts. Cell Mol Life Sci. 1997; 53:967–976. [PubMed: 9447250]

58. Rezvani HR, Mazurier F, Cario-Andre M, et al. Protective effects of catalase overexpression on UVB-induced apoptosis in normal human keratinocytes. J Biol Chem. 2006; 281:17999–18007. [PubMed: 16644728]

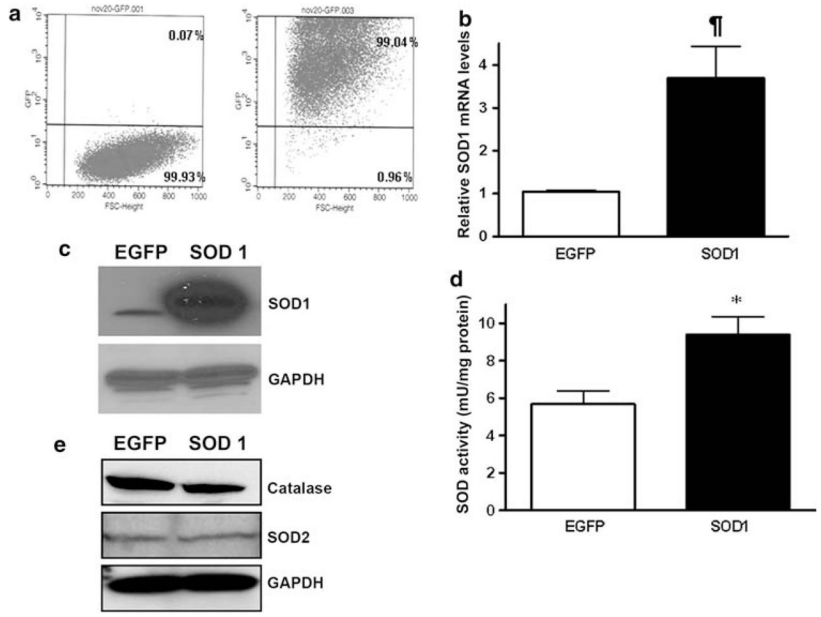

Fig. 1.

Genetic modification of LLC-PK$_1$ cells using lentiviral vectors. Vesicular stomatitis virus G (VSV-G) pseudotyped lentiviral vectors were used to transduce LLC-PK$_1$ cells to over-express green fluorescent protein (EGFP) and SOD1. **a** FACS analysis showing >99% EGFP transduction in LLC-EGFP cells (*right panel*) compared to wide type LLC-PK$_1$ cells (*left panel*) which served as a negative control. **b** Quantitative SOD1 mRNA level in LLC-SOD1 and LLC-EGFP cells by using real-time PCR. Results are means ± SEM. $N = 4$. ¶ $P < 0.01$ EGFP versus SOD1. **c** Western blots of SOD1 protein in a representative sample of LLC-SOD1 and LLC-EGFP cells. GAPDH served as the protein loading control. **d** SOD activity in LLC-SOD1 and LLC-EGFP cells by using superoxide dismutase assay kit. Results are means ± SEM. $N = 3$, * $P < 0.05$ EGFP versus SOD1. **e** Western Blot showing expression of SOD2 and catalase in LLC-EGFP and LLC-SOD1 cells

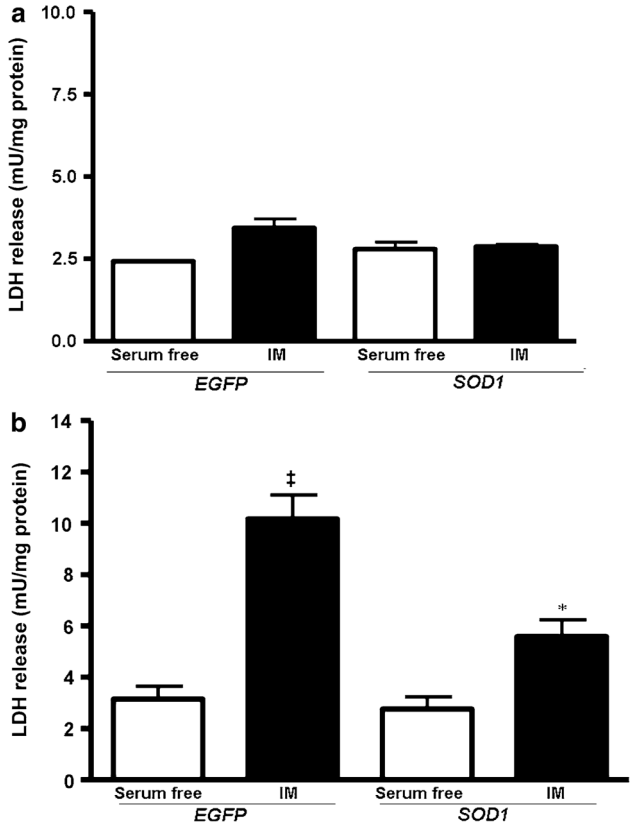

Fig. 2.

Cytotoxicity was assayed by measuring the lactate dehydrogenase (LDH) in media from LLC-SOD1 and LLC-EGFP cells after ATP depletion-recovery. **a** LDH levels in serum free and injured cells (IM) following 2 h ATP depletion and 2 h recovery (2–2 h). The results were not statistically significant from each other. **b** LDH release in serum free and injured cells (IM) following 4 h of ATP depletion and 2 h recovery. Results are means ± SEM. $N = 7$; ‡ $P < 0.001$ EGFP IM versus EGFP serum free, SOD1 serum free and SOD1 IM;* $P < 0.05$ SOD1 SF versus SOD1 IM

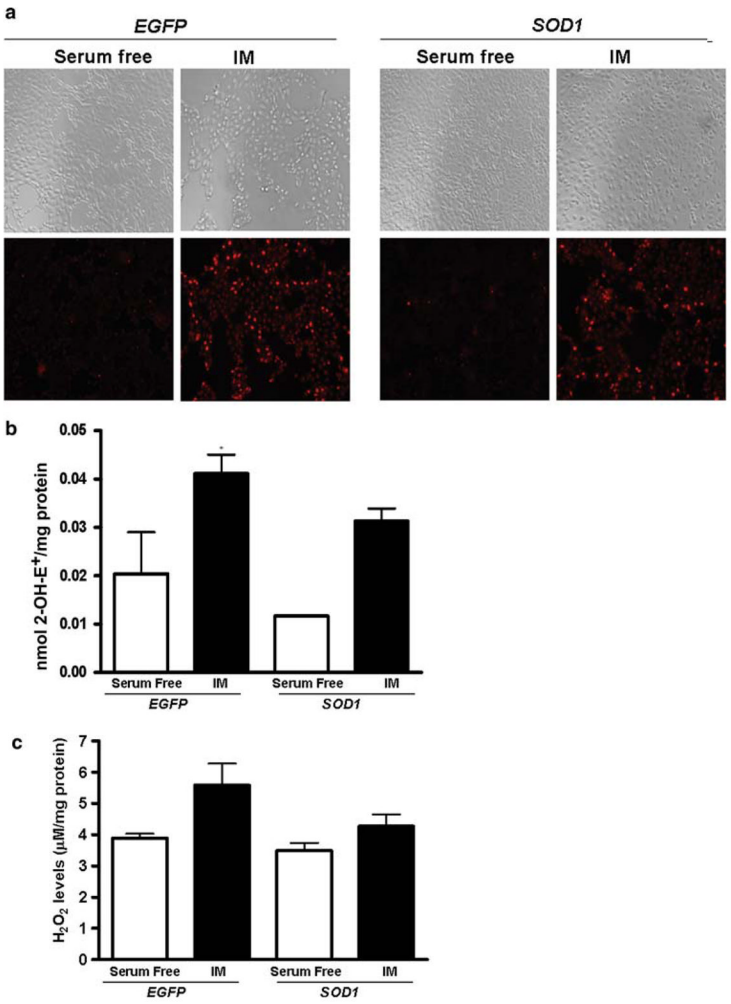

Fig. 3.

SOD1 over-expression decreased ROS levels. **a** Dihydroethidium (DHE) fluorescence images of LLC-SOD1 and LLC-EGFP cells after 4–2 h ATP depletion-recovery. *Upper panel* light microscopic images showed the total cell population in LLC-SOD1 and LLC-EGFP cells, SOD1 over-expression partially prevented the loss in total number of cells. *Lower panel* DHE fluorescent images, SOD1 over-expression partially reduced O2 $^{\bullet -}$ levels in response to ATP depletion injury. **b** Quantitation of $O_2{}^{\bullet -}$ measured by 2-OH-E^+ by HPLC using HE to measure intracellular superoxide level following 2–2 h injury. Results are means ± SE ($N = 3$ for all groups). * $P < 0.05$ EGFP IM versus EGFP serum free and SOD1 serum free. **c** H_2O_2 levels in LLC-EGFP and LLC-SOD1 cells after 4–2 h ATP depletion-recovery. Results are means ± SE ($N = 3$ per group). Results not statistically significant from each other

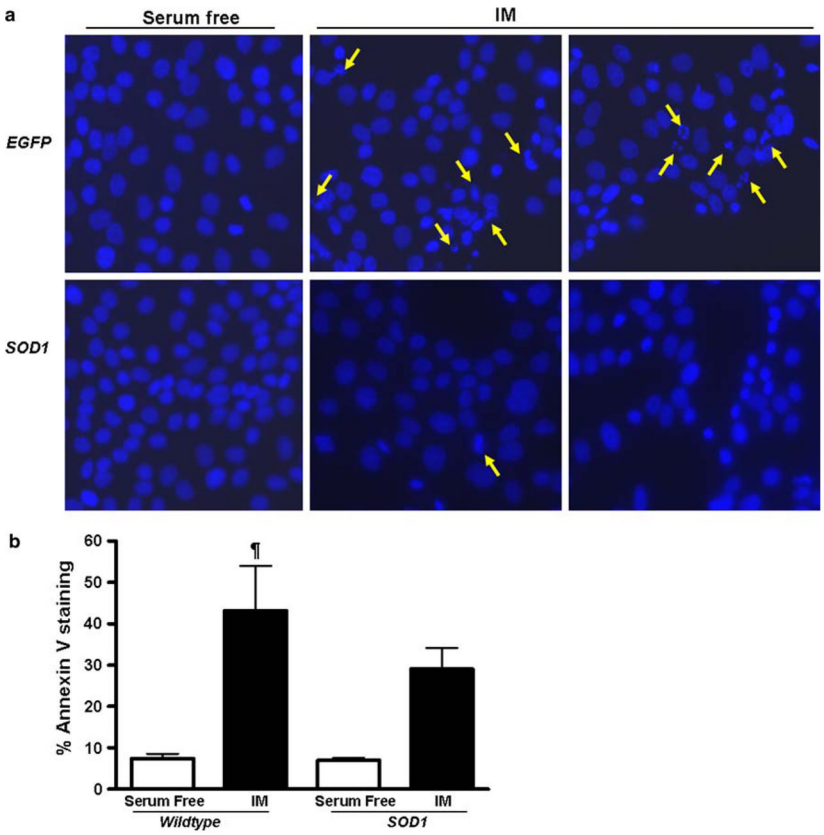

Fig. 4.

a Hoechst staining for nuclear morphology in LLC-SOD1 and LLC-EGFP cells following 4–2 h ATP depletion-recovery. *Panels* shown are representative images of individual LLC-EGFP and LLC-SOD1 cells under serum free and ATP depleted conditions (IM). Yellow arrows depict condensed and fragmented nuclei in the injured cells compared to the serum free controls. SOD1 over-expression preserved nuclear morphology following ATP depletion-recovery. **b** Apoptosis as measured by Annexin V staining and flow cytometry. *Open bars* are serum free and *black bars* are ATP depleted cells. Results are means ± SEM ($N = 3$ per group). ¶ $P < 0.01$ serum free (wild type and SOD1) versus IM (wild type)

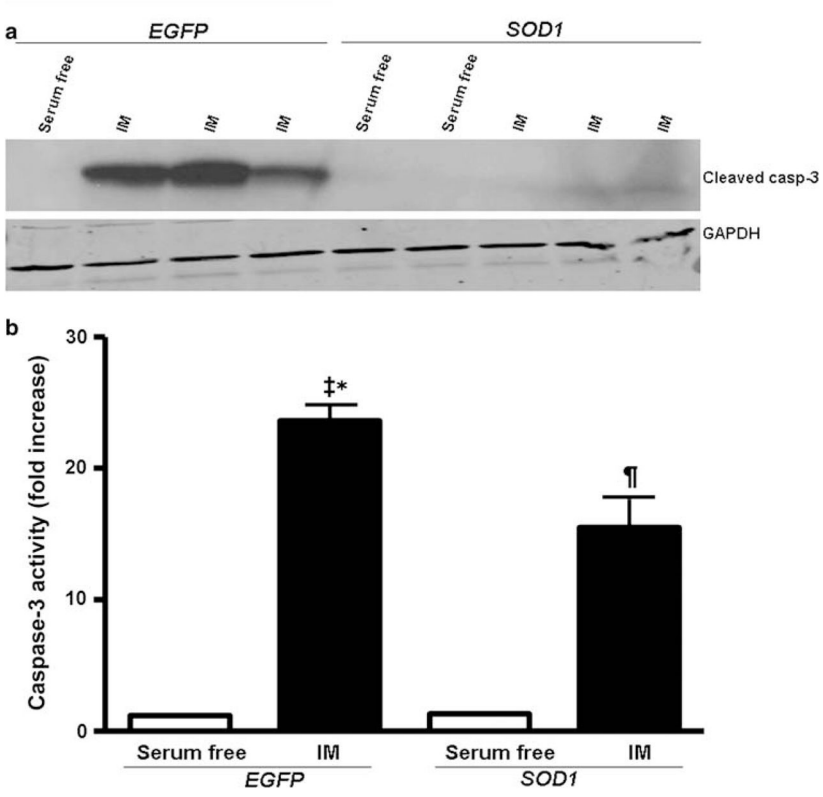

Fig. 5.

SOD1 over-expression partially decreases caspase-3 activation following ATP depletion-recovery. A. Western blots of activated cleaved caspase-3 and GAPDH in LLC-SOD1 and LLC-EGFP cells following 4–2 h serum free conditions or ATP depletion-recovery (IM). **b** Caspase-3 activity assay from LLC-SOD1 and LLC-EGFP cell lysates after 4–2 h ATP depletion-recovery. Results are means ± SEM. $N = 5–6$. ‡ $P < 0.001$ EGFP IM versus EGFP serum free and SOD1 serum free; ¶ $P < 0.01$ SOD1 IM versus EGFP serum and SOD1 serum free; * $P < 0.05$ EGFP IM versus SOD1 IM

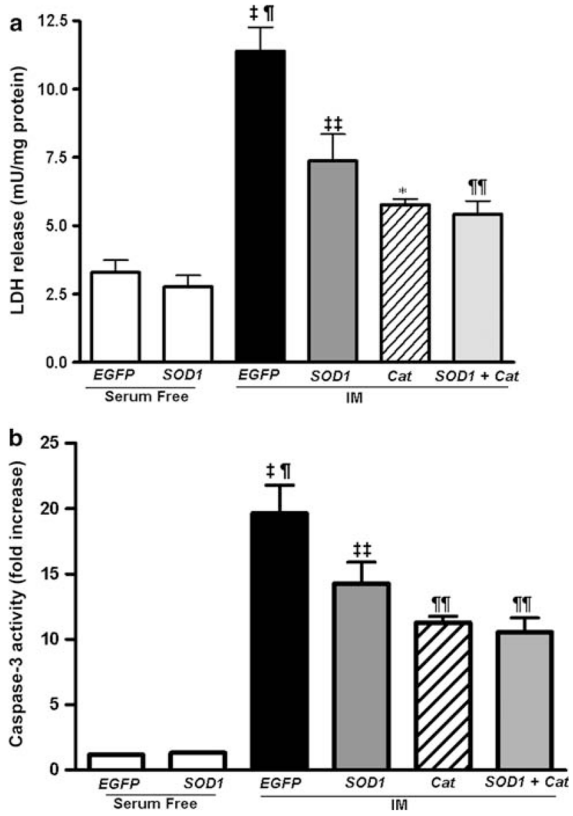

Fig. 6.

Effects of catalase on cytotoxicity and caspase-3 activity in ATP depleted LLC-EGFP and LLC-SOD1 cells. **a** LDH assay in LLC-SOD1 and EGFP cells with or without catalase following 4–2 h ATP depletion-recovery. Results are means ± SEM. $N = 4–9$. ‡ $P < 0.001$ EGFP IM versus EGFP serum free, SOD1 serum free; ¶ $P < 0.01$ EGFP IM versus SOD IM, Cat IM and SOD + Cat IM; ‡‡ $P < 0.001$ SOD IM versus EGFP serum free and SOD1 serum free; * $P < 0.01$ Cat IM versus EGFP IM, EGFP serum free and SOD1 serum free; ¶¶ P < 0.01 SOD + Cat IM versus EGFP SF and SOD1 SF. **b** Caspase-3 activity in LLC-SOD1 and EGFP cells with or without catalase following 4–2 h ATP depletion-recovery. Results are means ± SEM. $N = 3–9$. ‡ $P < 0.001$ EGFP IM and SOD1 IM versus EGFP serum free and SOD1 serum free; ¶ $P < 0.01$ EGFP IM versus SOD IM, Cat IM and SOD + Cat IM; * $P < 0.01$ Cat IM versus EGFP IM, SOD1 serum free and EGFP serum free; ¶¶ $P < 0.01$ SOD + Cat IM versus EGFP IM, SOD1 serum free and EGFP serum free

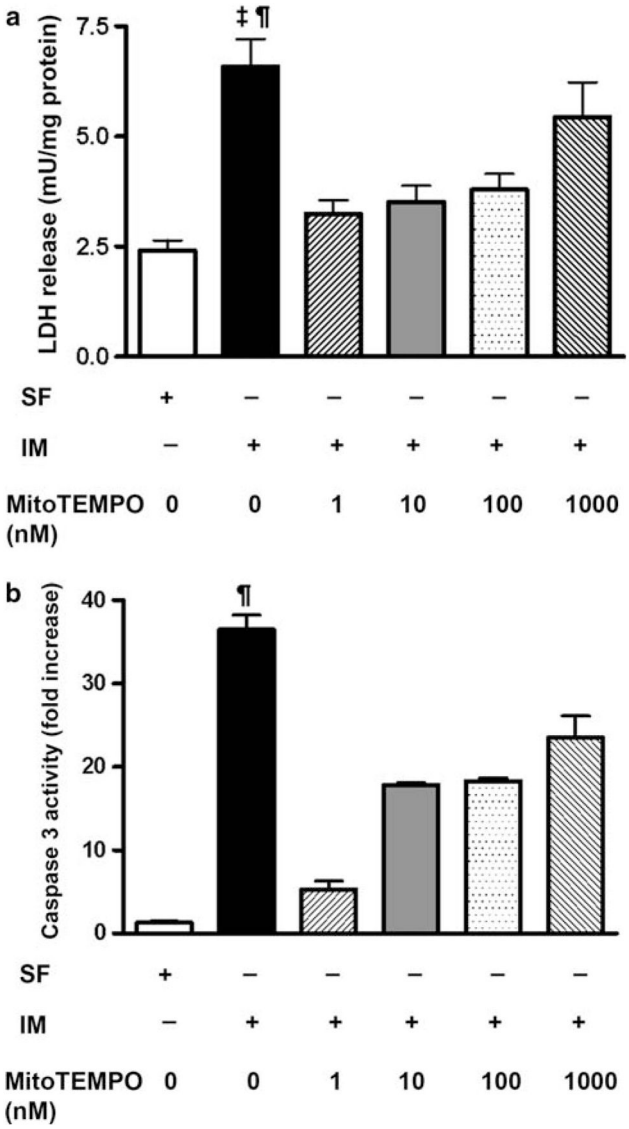

Fig. 7.

Effect of different doses of MitoTEMPO on cytotoxicity and caspase-3 activity in serum free (SF) LLC-PK1 cells and LLC-PK1 cells undergoing 4–2 h ATP depletion-recovery (IM). **a** LDH release in serum free, IM and MitoTEMPO treated cells. Results are means ± SEM. $N = 3–12$. ‡ $P < 0.001$ IM versus SF, MitoTEMPO 1 nM and MitoTEMPO 10 nM; ¶ $P < 0.01$ IM versus MitoTEMPO 100 nM. **b** Caspase-3 activity in serum free, IM and MitoTEMPO treated cells following 4–2 h ATP depletion-recovery. Results are means ± SEM ($N = 3$ per group). ¶ $P < 0.01$ IM versus all other groups